

Space charge limited avalanche growth in Multigap Resistive Plate Chambers

A.N. Akindinov⁶, A. Alici^{1,5}, F. Anselmo⁵, P. Antonioli⁵, Y. Baek^{4,7}, M. Basile^{1,5}, G. Cara Romeo⁵, L. Cifarelli^{1,5}, F. Cindolo⁵, F. Cosenza², A. De Caro², S. De Pasquale², A. Di Bartolomeo², M. Fusco Girard², M. Guida², D. Hatzifotiadou^{4,5}, A.B. Kaidalov⁶, D.W. Kim³, D.H. Kim^{4,7}, S.M. Kisselev⁶, G. Laurenti⁵, K. Lee³, S.C. Lee³, E. Lioublev⁶, M.L. Luvisetto⁵, A. Margotti⁵, A.N. Martemiyarov⁶, R. Nania⁵, F. Noferini¹, P. Otiougova^{4,7}, F. Pierella^{1,5}, P.A. Polozov⁶, E. Scapparone⁵, G. Scioli^{1,5}, S.B. Sellitto², A.V. Smirnitski⁶, M.M. Tchoumakov⁶, G. Valenti⁵, D. Vicinanza², K.G. Voloshin⁶, M.C.S. Williams^{4,5}, B.V. Zagreev⁶, C. Zampolli^{1,5}, A. Zichichi^{1,4,5}

¹ Dipartimento di Fisica dell'Università, Bologna, Italy

² Dipartimento di Fisica "E.R.Caianiello" dell'Università and INFN, Salerno, Italy

³ Department of Physics, Kangnung National University, Kangnung, South Korea

⁴ EP Division, CERN, Geneva, Switzerland

⁵ INFN Bologna, Bologna, Italy

⁶ ITEP, Moscow, Russia

⁷ World Laboratory, Lausanne, Switzerland

Received:

Abstract. The ALICE TOF array will be built using the Multigap Resistive Plate Chamber(MRPC) configured as a double stack. Each stack contains 5 gas gaps with width of 250 μm . There has been an intense R&D effort to optimise this new detector to withstand the problems connected with the high level of radiation at the LHC. One clear outcome of the R&D is that the growth of the gas avalanche is strongly affected by space charge. The effect of the space charge is a decrease in the rate of change in gain with electric field; this allows more stable operation of this detector. We have measured the gain as a function of the electric field and also measured the ratio of the fast charge to the total charge produced in the gas gap. It is well established that RPCs built with 250 μm gas gap have a much superior performance than 2 mm gaps; we discuss and compare the performance of 250 μm gap MRPCs with 2 mm gap RPCs to show the importance of space-charge limitation of avalanche growth.

PACS: 29.40.Cs; 7.77.-n; 52.80.Dy

1 Introduction

The Time-of-Flight array for the ALICE experiment is built using Multigap Resistive Plate Chambers (MRPC). Since exceptional time precision is needed, small gas gaps are employed. The final design, arrived at after a period of R&D, is to build a MRPC with 10 gas gaps, each with a width of 250 μm ; this is arranged as a double stack with each stack containing 5 gaps.

An important consideration with all parallel plate chambers is the precision required for the width of the gas gap. Since the ALICE TOF array covers an area of 150 m^2 , 1500 m^2 of gas gap will need to be constructed. The precision needed for the gas gap is thus an important parameter when considering mass production.

We will discuss the effect of space charge in the development of gas avalanches and show that this effect allows a relaxed tolerance on the gap width when small gas gaps ($\sim 250 \text{ }\mu\text{m}$) are used. In fact, for 2 mm gap RPCs tighter tolerances are needed.

2 Description and operation of a Multigap Resistive Plate Chamber

Figure 1 shows a schematic representation of a monogap RPC and a Multigap RPC. The gas volume in the multigap RPC is divided into a number of gas gaps with equal width (fig. 1 shows three such gaps) by inserting extra resistive plates. The voltage is applied by a resistive layer only to the external surfaces of the external plates; all the internal plates are electrically floating. Pickup electrodes are located outside the stack and insulated from the high voltage electrodes. Signals on the pickup electrodes are induced by the movement of charge; in the case of the RPC the fast signal is generated by the fast movement of electrons towards the anode. Since these resistive plates act as dielectrics, induced signals can be caused by the movement of charge in any of the gas gaps between the anode and cathode pickup electrodes. In this way the observed induced signal is the sum of charge movement in any of the gaps making up the multigap RPC.

Applying a high voltage to the anode and cathode electrodes generates an electric field in the gas gaps. Charged particles passing through this chamber will leave a trail of clusters of ionisation. These electrons will avalanche toward the anode according to Townsend equation $N = N_0 e^{\alpha x}$. N_0 is the number of electrons in the initial ionisation cluster; α is the Townsend coefficient and is equal to $1/\lambda$, where λ is the average distance between ionising collisions; x is the distance that the avalanche has traveled from the initial position of the ionising cluster. The electrons produced by the avalanche induce a fast signal as they move toward the anode; a much slower signal is produced by the positive ions as they drift toward the cathode. The ratio of the fast signal to the total signal is $1/\alpha D$ for a gap of width D .

If the number of electrons in the avalanche increases above $\sim 10^8$, the transition to a streamer can be initiated. Thus an RPC operated in “avalanche” mode, one uses an electric field such that the maximum gain ($\sim \exp(\alpha D)$) does not exceed 10^8 . Therefore the maximum value of αD is ~ 18 and the ratio of fast signal to total is, $1/\alpha D$, $\sim 5\%$. The fast signal is processed by the front-end electronics to generate a ‘hit’; but it is the total charge produced in the gap by the avalanche that has to flow through the resistive plates and is responsible for the limited rate capability of RPC. Obviously for high rate applications we need to minimise the total charge produced in the gas gap.

The gas avalanche process discussed above will generate electrons that flow into the anode and an equal charge of positive ions into the cathode plate. If

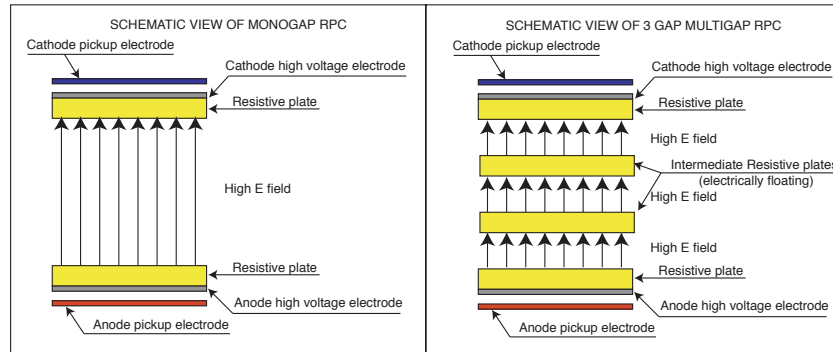


Fig. 1. Schematic representation of monogap and multigap RPC.

the multigap resistive plate chamber has equally sized gas gaps and the voltages on the floating internal plates is arranged so that there is the same potential difference across each gap, then each internal resistive plate will have a flow of electrons into one surface and an equal flow of positive ions into the opposite surface; thus the net flow of charge into a ‘floating’ resistive plate will be zero. This is the stable state. If, however, the voltage on one of these internal plates changes to an incorrect value, then the potential difference across two neighbouring gaps will be altered. In this case the flow of electrons from one gas gap will not be equal to the flow of positive ions from the next gas gap, so there will be a flow of charge into this resistive plate. It is easy to show that this flow of charge will be such to move the potential on the resistive plate to the ‘correct’ value. Thus the voltage on the floating plates is self-regulation with equal gas gain in all gaps of the multigap RPC being the stable condition.

3 The MRPC with a heavy, electronegative gas

If the RPC is operated with an electronegative gas then an electron has a chance of being captured by a molecule (thus forming a negative ion). In this case the number of positive ions is equal to the number of ‘free’ electrons plus the number of negative ions; however the fast signal is still only due to the movement of the electrons. The ratio of fast signal to the total is still $1/\alpha D$; however the avalanche growth is governed by the effective Townsend coefficient, $\alpha_{eff} = \alpha - \eta$ where α is the Townsend coefficient; η is the attachment coefficient and D is the gap width. Therefore the ratio of fast to total is $1/(\alpha_{eff} + \eta)D$. One can see that the current due to the slow moving ions is substantially increased if η is large and therefore the use of electronegative gasses cause a degradation in the rate capability.

For an RPC working in avalanche mode, the applied voltage is chosen so that a single electron crossing the complete gap has a gas gain of $\sim 10^8$. This number of electrons is the threshold for streamer production; thus higher applied voltages would produce an unacceptable fraction of streamers. An avalanche started by an electron at a position 25 % of the gap width away from the cathode would

create an avalanche that has 10^6 electrons; since the fast signal/total signal is $1/\alpha \cdot D$ ($\approx 5\%$), this avalanche with 10^6 electrons would generate a fast signal of 8 fC. Such a signal is small especially as RPCs are used as trigger devices covering a large area. Thus only the clusters created within 25 % of the total gap width close to the cathode will create avalanches of sufficient magnitude to induce detectable signals on the pick-up electrodes.

A typical (light) gas used in gaseous chambers is Argon. On average, a minimum ionizing particle creates 3 clusters of ionization per mm of path length. Thus for a 2 mm gap RPC one would have an average of 1.5 clusters capable of growing avalanches that can generate a detectable signal. This implies that the efficiency of a 2 mm gap RPC filled with a light gas and operated in ‘avalanche’ mode would be $(1 - \exp(-1.5)) \times 100 = 78\%$. For this reason gas of high density needs to be used. Since in many applications one has to use a non-flammable gas, only a small fraction of hydrocarbon gas can be used. Therefore freons such as $C_2F_4H_2$ (Suva 134a) are widely used; they are heavy and non-flammable. Such a gas as Suva 134a is 2.5 denser than argon; this leads to an efficiency of 98 % for a single 2 mm gap RPC following the arguments presented above. Most freons are, however, electronegative.

In fig. 2 we show the Townsend coefficient, α , the attachment coefficient, η , and the effective Townsend coefficient, α_{eff} for a gas mixture of 95 % $C_2F_4H_2$ and 5 % $i-C_4H_{10}$. These values are obtained from the program MAGBOLTZ[6, 7]. As stated above one normally operates RPCs in avalanche mode with an electric field corresponding to α_{eff} of 10. As can be seen from the figure, this occurs at a field of 47 kV/cm. If the applied voltage is varied by $\pm 1\%$ the gas gain will change from $1 \cdot 10^8$ to $2 \cdot 10^9$ (i.e. a factor 20). It is not surprising, therefore, that the ‘standard’ RPC with a 2 mm gap has a very short ‘streamer-free’ efficiency plateau (where the limits are defined at the low side by a drop in efficiency and the high side by the onset of streamers).

4 The fast and slow component of the induced signal

The measurement of the slow current and the measurement of the ratio of the fast signal to the total is relatively straightforward. In fig. 3 we show such a measurement reported in ref. [8]. For the avalanche represented by fig. 3 the ratio of fast/total signal is $2.3/15.4 = 0.15$, somewhat higher than expected.

This ratio increases substantially in the case of a MRPC. In fig. 4 we show a signal from a 10 gap MRPC with 250 μm gaps as used for the ALICE TOF detector [3] (i.e. double stack, with each stack using 4 internal glass plates of 400 μm thickness, 2 external glass plates of 550 μm thickness; all glass is ‘soda-lime’ float glass). It is clear that the slow voltage ramp due to the movement of positive ions towards the cathode is non-linear. The ramp deviates from linear behaviour between 500 and 600 ns after the formation of the avalanche for a total drift time of the positive ions of 1.2 μs . One would expect a linear behaviour if the positive ions were all located at some point (such as the case where the avalanche grew exponentially as defined by Townsend). This non-linear behaviour indicates that the positive ions are spread over a distance. Since deviations from the linear ramp becomes apparent after half the total drift time for the positive ions, one

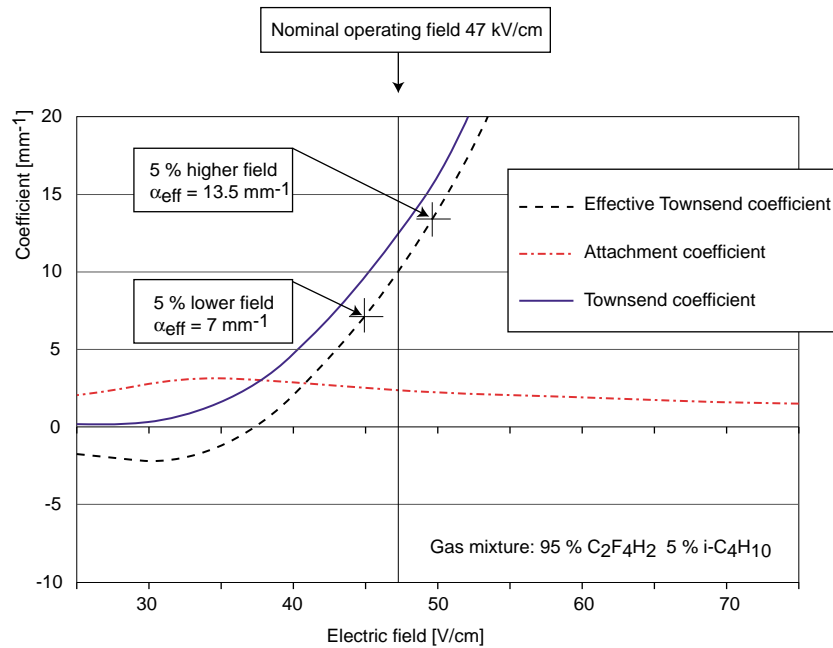


Fig. 2. Townsend coefficient, attachment coefficient and effective Townsend coefficient plotted versus electric field for a gas mixture of 5 % isobutane and 95 % $\text{C}_2\text{F}_4\text{H}_2$. The 2 mm gap RPC is normally operated with an effective Townsend coefficient of 10, corresponding to an electric field of 47 kV/cm. The value of effective Townsend coefficient for a change of electric field of ± 5 % are marked on this figure.

can conclude that the positive ions are spread over half the total gap size of $250 \mu\text{m}$. The reason for this is space charge of the positive ions. As the avalanche grows, the electrons at the ‘head’ of the avalanche experience a reduced electric due to the charge of the positive ions in the tail of the avalanche. Therefore the electrons experience a lower electric field and the gas gain is reduced, thus the avalanche deviates from exponential growth. By this means the centre of gravity of the production of the electrons (and positive ions) moves away from the anode; this will cause an increase in the ratio of fast charge versus the total charge. This ratio should increase for large avalanches where space charge effects become more important. In fact this is what we observe and is shown in fig. 5. Thus we see evidence that ‘space-charge limited’ avalanche growth (saturated avalanche growth) both in the ratio of fast charge to total charge and with the time development of the induced voltage caused by the drift of the positive ions.

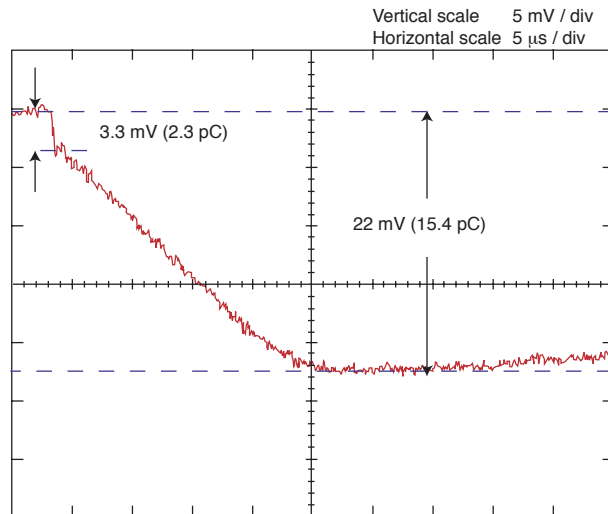


Fig. 3. Induced charge caused by charged particle passing through a 2 mm gap RPC. The readout electrodes were connected to the high impedance input of a digital oscilloscope so that the voltage represented the total collected charge at that point. By knowing the capacitance, the correspondence between voltage and charge is given. Details can be found in ref. [8]

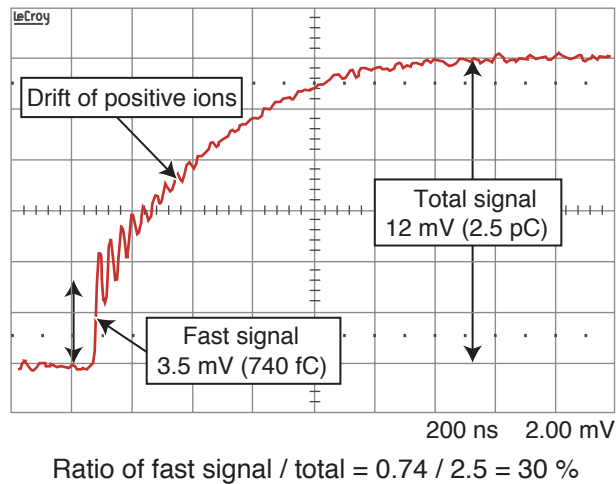


Fig. 4. Induced charge caused by charged particle passing through a 10 μm gap RPC with gap size of 250 μm. The readout electrodes were connected to the high impedance input of a digital oscilloscope so that the voltage represented the total collected charge at that point. By knowing the capacitance (212 pF in this case), the correspondence between voltage and charge is given.

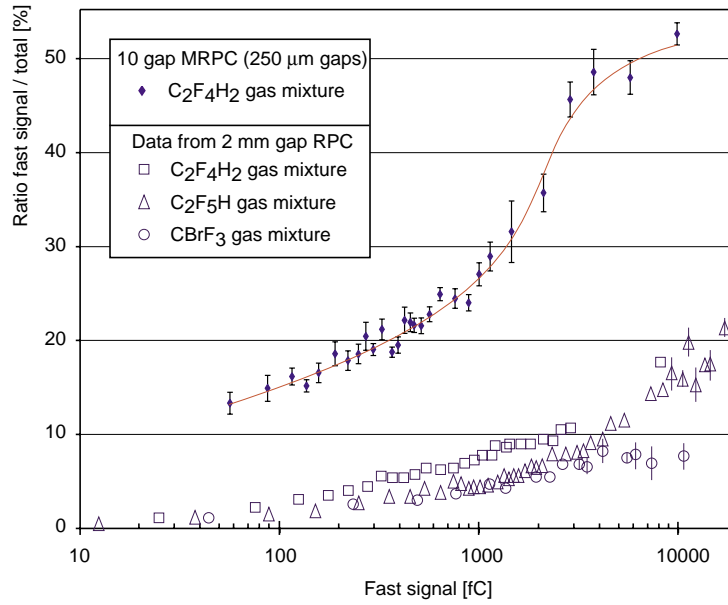


Fig. 5. Ratio of fast induced charge to the total induced charge plotted as a function of increasing fast charge.

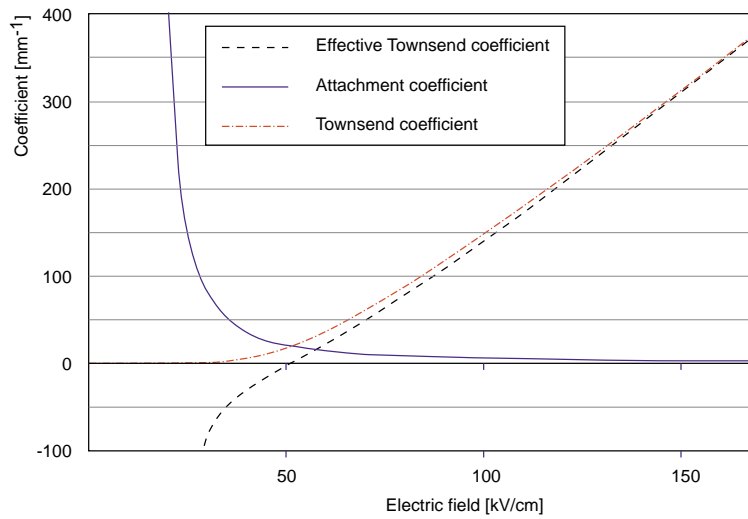


Fig. 6. Townsend, attachment and effective Townsend coefficient as a function of electric field for a gas mixture 90 % $C_2F_4H_2$, 5 % SF_6 , $i-C_4H_{10}$

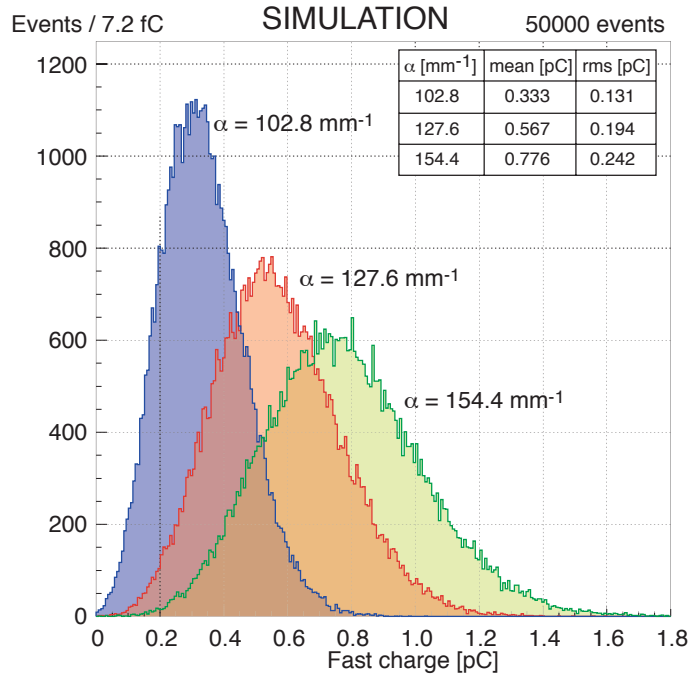


Fig. 7. Simulated charge spectra for a 10 gap MRPC using the model of Riegler et al. [4]. The value of $\alpha = 127.6 \text{ mm}^{-1}$ is obtained from MAGBOLTZ (see fig. 6). Distributions for also shown for $\alpha = 102.8$ and 154.4 mm^{-1} .

5 Avalanche growth in small gas gaps

We have worked extensively with 10 gaps MRPCs where the gap width is $250 \mu\text{m}$. A typical applied voltage is 12 kV across 5 gas gaps; this corresponds to an E field of 96 kV/cm. The Townsend (α), attachment (η) and effective Townsend ($\alpha_{eff} = \alpha - \eta$) are plotted as a function of electric field in fig. 6 for the gas mixture 90 % $\text{C}_2\text{F}_4\text{H}_2$, 5 % $\text{i-C}_4\text{H}_{10}$ and 5 % SF_6 . Riegler et al. [4] have discussed space charge effects and propose a model where the avalanche simply stops growing when the number of electrons reached some limit ($1.6 \cdot 10^7$); these electrons drift to the anode without any further multiplication. Using this model with the $1.6 \cdot 10^7$ limit for the avalanche limit together with the Townsend coefficient and attachment coefficients predicted by MAGBOLTZ, we have simulated the expected fast charge distribution from the 10 gap MRPC as will be used for the ALICE TOF. This is shown in fig. 7 together with a distributions generated with α varied by $\pm 20 \%$.

The distributions shown in fig. 7 are with a maximum avalanche size set to be $1.6 \cdot 10^7$. Varying this parameter changes the mean value of the fast charge, but does not change the shape of the charge spectrum. However varying α does change the shape and the spectrum becomes narrower with increasing α . Thus if we try to fit a measured charge spectra (measured with 7 GeV/c pions) to the

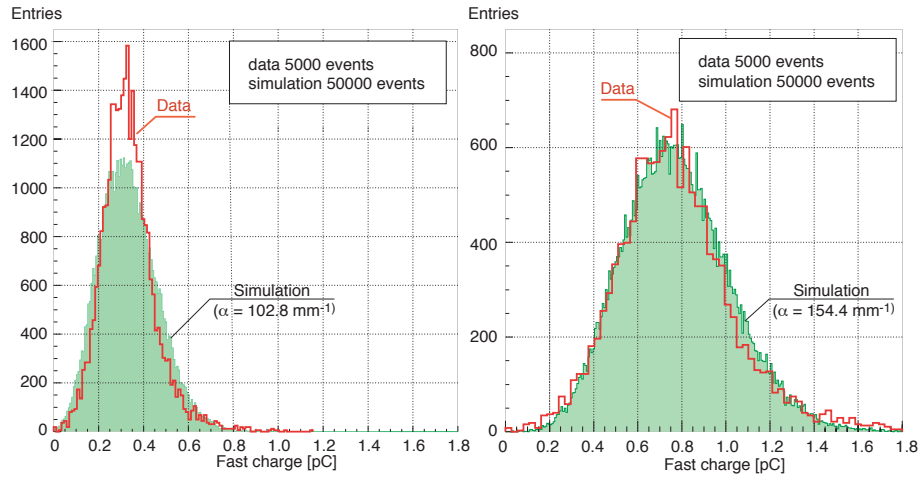


Fig. 8. Distributions from fig.7 with a measured distribution obtained with 7 GeV/c pions superimposed. It is clear that the data matches well with the simulation using $\alpha = 154.4 \text{ mm}^{-1}$.

simulated charge spectra, by matching the means of the two distributions, one finds that the data does not fit with the simulation when a value of $\alpha = 102.8 \text{ mm}^{-1}$ is used. This is shown in fig. 8. However the agreement between simulation and data is impressively good if $\alpha = 154.4 \text{ mm}^{-1}$ is used.

It is clear that this rather simplified description of space-charge limiting avalanche growth as proposed by Riegler et al. [4] models the data exceptionally well. It is also clear that the only way of obtaining a charge distribution as measured from the 10 gap MRPC destined for the ALICE-TOF is to start the avalanche development with these very high values of effective Townsend coefficient. The preferred value of α is $\sim 20 \%$ higher than predicted by MAGBOLTZ

A decrease in the size of the $250 \mu\text{m}$ gas gap will cause the electric field to increase and therefore also the effective Townsend coefficient, thus an electron starting at the cathode reaches this space charge saturation of $1.6 \cdot 10^7$ sooner. However now the gas gap is smaller so that the avalanche is terminated sooner. In this way the increase in the gas gain produced by decreasing the gap size is balanced by the decrease in the induced signal due to shorter distance to the anode. With a gap width of $250 \mu\text{m}$ and with this gas mixture, we find these effects balance. We show this in fig. 10.

6 Discussion

We have observed the effect of space charge by: (a) the non-linear ramp of induced charge by the positive ions, (b) the large values of the ratio of fast charge to total charge and the increase of this ratio with charge and (c) the excellent agreement between the measured charge spectra and simulated charge spectra as predicted by the model of Riegler [4].

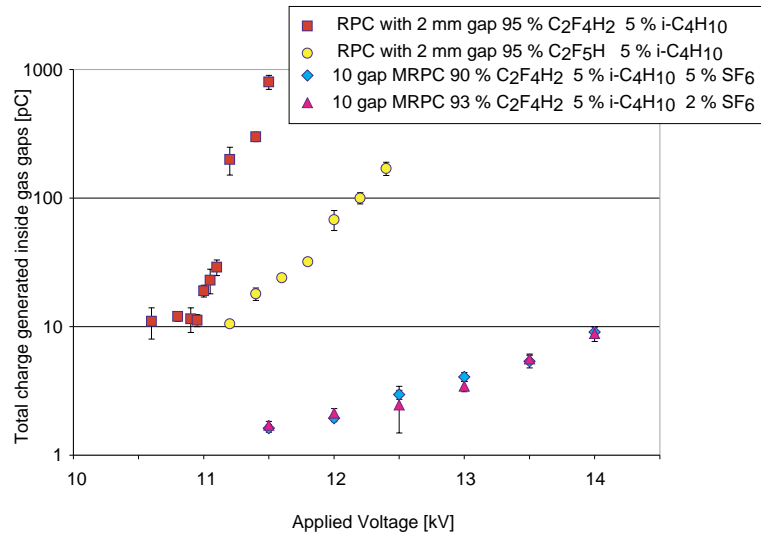


Fig. 9. Total charge produced in gas gaps versus applied voltage. In the case of the 2 mm gap RPC, the voltage is applied across the single gap. The MRPC is for a double stack MRPC with 10 gaps of 250 micron. The voltage shown is the voltage applied across 5 gas gaps.

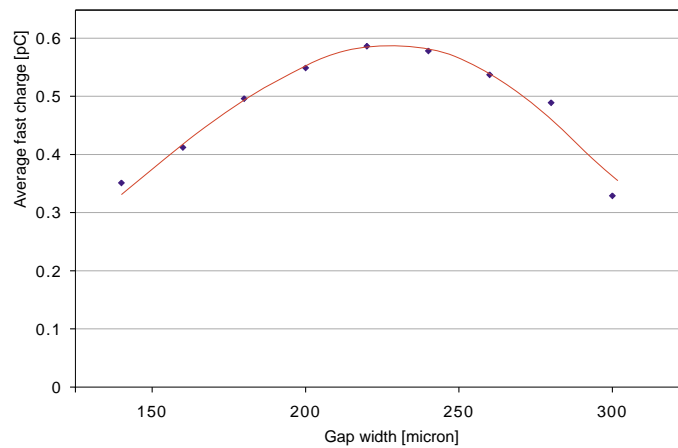


Fig. 10. Simulation of the average charge versus gap width for a ten gap double-stack MRPC, with a fixed voltage of 12 kV across 5 gas gaps using a Townsend coefficient calculated by the MAGBOLTZ program and a limit of avalanche growth set at $1.6 \cdot 10^7$ electrons (see text for details).

Space charge effects play a very important role and limit the growth of the avalanche to be a size just prior to streamer production. This limitation in avalanche growth also leads to a less rapid change in gain with applied voltage; thus one can work in avalanche mode relatively free of streamers even at 2 kV above the knee of the efficiency plateau.

The ratio of fast charge to total charge is also enhanced by this space charge effect and typically the MRPC with small gas gaps is operated at a factor 10 to 20 less charge being produced in the gas gaps than a 2 mm RPC with a single gap. This will lead to an enhanced rate capability (that we have previously measured [9]) and a large reduction in any ageing effects.

References

1. E. Cerron Zeballos, I. Crotty, D. Hatzifotiadou, J. Lamas Valverde, S. Neupane, M.C.S. Williams and A. Zichichi, Nucl. Instr. Meth. A374(1996)132.
2. ALICE Technical Design Report of the Time of Flight System, CERN/LHCC 2000-012 ALICE TDR 8, 16 February 2000.
3. ALICE Time of Flight Addendum, CERN/LHCC 2002-016 Addendum to ALICE TDR 8, 24 April 2002.
4. W. Riegler, C. Lippmann, R. Veenhof, Nucl. Instr. Meth A500(2003)144.
5. E. Cerron Zeballos, I. Crotty, D. Hatzifotiadou, J. Lamas Valverde, R.J. Veenhof, M.C.S. Williams and A. Zichichi, Nucl Instr Meth A381(1996)569.
6. S. Biagi, Nucl. Instr. Meth. A283(1989)716.
7. S. Biagi, Nucl. Instr. Meth. A421(1999)234.
8. E. Cerron Zeballos, I. Crotty, D. Hatzifotiadou, J. Lamas Valverde, M.C.S. Williams and A. Zichichi, Nucl. Instr. Meth. A 396(1997)93.
9. A. Akindinov et al. Nucl. Instr. Meth. A 490(2002)58.